3-D radio-frequency CSEM at the Weidenpesch waste site in Cologne

M. Smirnova[1], B. Tezkan[1], A. Shlykov[2], S. Fadavi[1], A. Saraev[2], P. Yogeshwar[1]
[1]University of Cologne, maria.smirnova@uni-koeln.de
[2]Saint-Petersburg State University

Summary

A classical radio-magnetotelluric (RMT) method is routinely applied to various environmental, engineering, and exploration problems. The technique uses the radio-transmitters broadcasting electromagnetic fields at frequencies above 10 kHz. A significant disadvantage of RMT is a lack of robust radio transmitters in remote areas and a limited depth of investigation. To overcome these problems, the controlled sources can be used as an active source – the CSRMT method. Such modification allows measurements in remote areas and the extended frequency range (from 1 kHz to 1 MHz). However, with controlled sources, maintaining the plain-wave assumption at all frequencies and throughout the survey area is often problematic. In this contribution, we present an implementation of the CSRMT method with sources installed in the survey area (near-to-far-field zones). This is, in fact, a CSEM method working in the radio-frequency band. However, we consider impedance tensor and tipper vector transfer functions, which require measurement and modelling of two source polarisations. Here, we present the results of the radio CSEM measurements collected at the Weidenpesch waste site in Cologne. In the obtained 3-D model, the waste site is well resolved. The model agrees with the boreholes' interpretation and the area's known geology.

Keywords: CSRMT, CSEM, 3-D inversion, Weidenpesch waste site

Introduction

The concept of using controlled sources (CS) to improve the data quality and depth of investigation of AMT and RMT methods has earlier shown its potential (Hughes&Carlson 1987; Bastani 2001). There, sources were installed in the far-field to fulfil the plane-wave assumption. One of the disadvantages of such far-field CSAMT/CSRMT (Saraev et al 2017) is that there are still some source effects in the data (Li&Pedersen 1991), or if the source is too far, the signal-to-noise ratio decreases substantially. Here, we present the CSRMT method, with sources installed in the survey area (measurements in near-to-far-field zones), which is, in fact, a CSEM method working in the radio-frequency band. In this case, the source geometry must be considered during modelling. We have implemented the modelling and inversion for the 3-D case using our finite-difference code in Matlab (Egbert et al., 2017, Cherevatova et al., 2018). We consider two perpendicular sources (horizontal electric dipole (HED) lines) to estimate the impedance tensor and tipper vector transfer functions. Such an approach avoids measurements of the current strength time series, which is difficult at high frequencies.

Several CSRMT field surveys have been conducted to verify the method. Here, we present the results of the CSRMT survey over the Weidenpesch waste site in Cologne, Germany. This area was selected because the conductive waste site is buried in a contrasting, more resistive host rock. The geology of the sub-surface, composition and history of the waste site is well known. The waste site is about 400 m by 90 m in lateral size and about 10 m thick. It comprises various building debris, household wastes, dust, grinding, and stone materials and is surrounded by relatively resistive gravel and sand. The site is closed and covered with a thin layer of fine silty sand (0.5-2.5 m thick). In addition to CSRMT measurements, ERT, magnetic and TEM data were acquired and will be used later for comparison.

Methods

The 3-D radio-frequency CSEM modelling and inversion was implemented within the MR3DMod framework – an object-oriented code in Matlab. The code was initially created as a prototype of MT ModEM software (Egbert&Kelbert 2012, Egbert et al. 2017), later extended for other methods, e.g., CSEM, TEM, DC, gravity and magnetics. Thus, as in ModEM, the modelling is performed using finite-difference approximation on a staggered grid. For CSEM, we followed the scattered-field approach (Newman&Alumbaugh 1995), where the total field (we solve for $\mathbf{E}$ field) is split into the background and anomalous (scattered) parts: $\mathbf{E} = \mathbf{E}_b + \mathbf{E}_a$. The background EM field is calculated using 1-D quasianalytical code of Key (2009). The anomalous field is calculated by solving a system of partial equations:

$$\nabla \times \nabla \times \mathbf{E}_a + i\omega\mu_0\sigma\mathbf{E}_a = -i\omega\mu_0(\sigma - \sigma_b)\mathbf{E}_a, \quad (1)$$

where the right-hand side is an external source term, μ_0 is the magnetic permeability of free space, ω is the angular frequency, and σ_b is the background conductivity (1-D half-space). In this study, we neglect the displacement currents as the sub-surface's resistivity is below 1000 Ωm, and there is no evidence of the strong polarisation effects in the field example discussed later. Once the solution for the anomalous electric field is obtained, the anomalous magnetic field is computed as

$$\mathbf{H}_a = \frac{1}{i\omega\mu_0}\nabla \times \mathbf{E}_a. \quad (2)$$

The total magnetic field is then calculated as a superposition of the background field and anomalous field: $\mathbf{H} = \mathbf{H}_b + \mathbf{H}_a$. Equations 1 and 2 are calculated twice, once for each source polarisation. Then, EM fields are interpolated from grid edges/faces to the site locations, and impedance tensor or tipper vector transfer functions are estimated. The subsequent procedure for calculating the Jacobian is the same as in Egbert&Kelbert 2012 with a non-zero source (CSEM and adjoint cases). For inversion, we used the data space-Occam method (Siripunvarapon et al. 2004).

Results

The Weidenpesch survey was conducted in two phases. The first phase was CSRMT/RMT far-field measurements. The second phase, discussed in this contribution, was the transition zone CSRMT (Figure 1). Two perpendicular HED sources (Tx1 – 215 m, Tx2 – 465 m) were installed in the survey area. Source current was variable between 1 A and 7.5 A. Measurements were performed along a set of profiles (red circles in Figure 1) crossing the waste site (dashed grey line in Figure 1). The distance between profiles is about 30 m and between sites about 10 m. At each site, six recordings were done, three for each source at base frequencies of 0.5, 5, and 50 kHz, to cover the complete frequency range from 1 kHz to 1 MHz. The data were processed using the KMSProMT software (Smirnov 2003), which was adopted for CSEM processing by adding the discrete frequency selection (Smirnova et al. 2019).

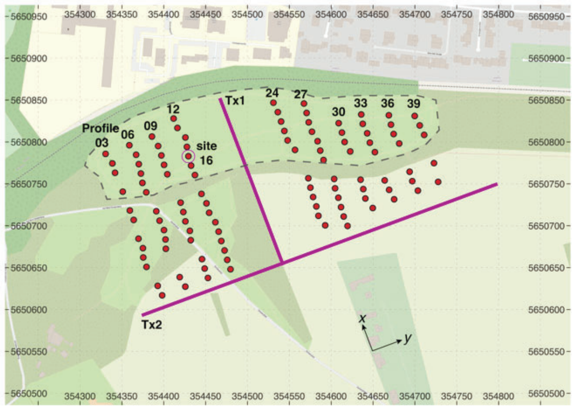

Figure 1. Survey plan for CSRMT measurements in the transition zone at Weidenpesch, Cologne. Red circles mark the location of the receivers; magenta lines are source locations. The waste site is outlined with a dashed grey line. Local coordinate system *xy* is shown on the map.

Figure 2 shows a pseudo-section of the *yx* component of the apparent resistivity and impedance phase for profile 12 (Figure 1). The apparent resistivity ranges from around 1 Ωm to 1000 Ωm. There is a clear boundary between the conductive waste site in the NW of the profile and the resistive background in the SE. The data are consistent from site to site and with a period, indicating good data quality.

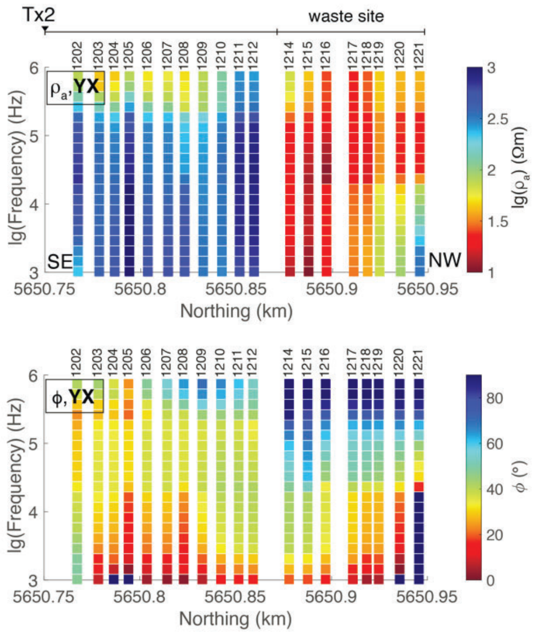

Figure 2. Pseudo-section of the *yx* apparent resistivity (top) and impedance phase (bottom) at profile 12 (see location in Figure 1).

In Figure 3, an example of a typical sounding curve at the waste site is shown (site 16 along profile 12 in Figure 1).

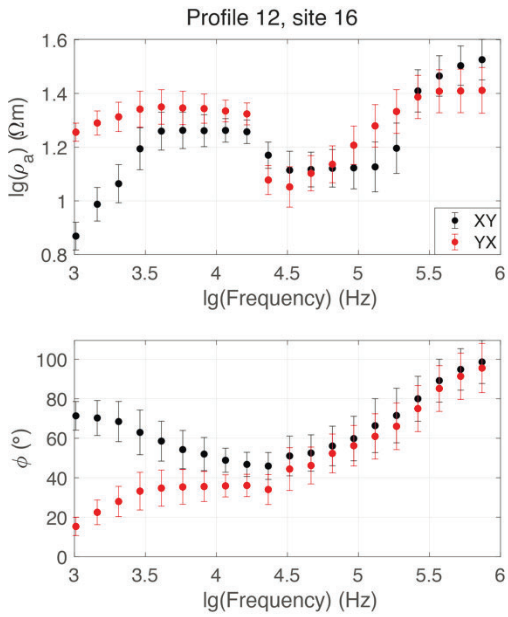

Figure 3. Apparent resistivity and impedance phase of the off-diagonal components of the impedance tensor at the selected site (see location in Figure 1).

In Figure 3, the *xy* slices from the 3-D model are shown at different depths (1 m, 2.1 m, 3.3 m, and 9.5 m). The model was obtained after inverting the impedance tensor at 114 sites in the frequency range from 1 kHz to 524 kHz. Error levels were set at 5% $\sqrt{|Z_{xy}Z_{yx}|}$ for all impedance components. The coordinate system was rotated by $20°$ to reduce the mesh size. The modelling domain was then discretised into 96x96x50 cells with a minimum 11 m cell size in the *x*-direction, 6 m in the *y*-direction and 1 m in the *z*-direction. A half-space of 50 Ωm was used as the initial model. The inversion converged to an RMS of 2.5.

Discussion

The highly conductive (1-10 Ωm) waste site is well resolved in the 3-D model (see slice at a depth of 3.3 m in Figure 4). The top of the anomaly is at a depth of around 2 m, and its thickness is about 7 m. The waste is covered by a resistive layer of fine silty sand (up to 1000 Ωm and about 1 m thick). The waste is underlain by a more resistive layer of gravel and sand (around 100 Ωm). This layering structure agrees with borehole interpretations, suggesting the top 2 m layer of fluviatile clays, underlain by a 20 m thick Pleistocene gravel and sand layer.

Conclusions

We presented a radio-frequency CSEM method (CSRMT in the transition zone) in this contribution. We developed and tested an algorithm for CSRMT 3-D modelling and inversion for the case when data are acquired in the vicinity of the source. Such an approach allows us to extend the measurement frequency range, depth of investigation and improve the signal-to-noise ratio. Additionally, it simplifies the survey planning and logistics, as sources can be installed directly in the survey area. We presented a real-field case study for the Weidenpesch waste site in Cologne. The 3-D model clearly outlines the waste site's location and shape and agrees with borehole data and geology.

Acknowledgements

The project was funded by the German Research Foundation (DFG) under grant number TE 170/21-1 and by the Russian Science Foundation, project number 21-47-04401.

References

Bastani M (2001) EnviroMT: A new controlled source/radio magnetotelluric system. PhD thesis, Uppsala University, Uppsala

Cherevatova M, Egbert GD, Smirnov MY (2018) A multi-resolution approach to electromagnetic modelling. Geophysical Journal International 214: 656—671

Egbert GD, Kelbert A (2012) Computational recipes for electromagnetic inverse problems. Geophysical Journal International 189: 251—267

Egbert GD, Smirnov MY, Cherevatova M (2017) Development of Flexible Object-Oriented MATLAB Codes for 3D EM Modeling. 6th International Symposium on Three-Dimensional Electromagnetics, Expand Abstr.

Hughes L, Carlson N (1987) Structure mapping at Trap Spring Oil eld, Nevada, using controlled-source magnetotellurics. First Break 5(11)

Key K (2009) 1D inversion of multicomponent, multifrequency marine CSEM data: Methodology and synthetic studies for resolving thin resistive layers. Geophysics 74: F9—F20

Li X, Pedersen LB (1991) Controlled source tensor magnetotellurics. Geophysics 56: 1456–1461

Newman GA, Alumbaugh DL (1995) Frequency-domain modelling of airborne electromagnetic responses using staggered finite differences. Geophysical Prospecting 43: 1021—1042

Saraev A, Simakov A, Shlykov A, Tezkan B (2017) Controlled source radiomagnetotellurics: A tool for near surface investigations in remote regions. Journal of Applied Geophysics 146: 228—237

Siripunvaraporn W, Uyeshima M, Egbert G (2004) Three-dimensional inversion for network-magnetotelluric data. Earth, Planets and Space 56: 893—902

Smirnov MY (2003) Magnetotelluric data processing with a robust statistical procedure having a high breakdown point. Geophysical Journal International 152: 1—7

Smirnova M, Becken M, Nittinger C, Yogeshwar P, Moerbe W, Rochlitz R, Steuer A, Costabel S, Smirnov MY, DESMEX Working Group (2019) Three-dimensional inversion of semi-airborne data from the flight experiment over an ancient mining area near Schleiz, Germany. Geophysics 84: E281—E292

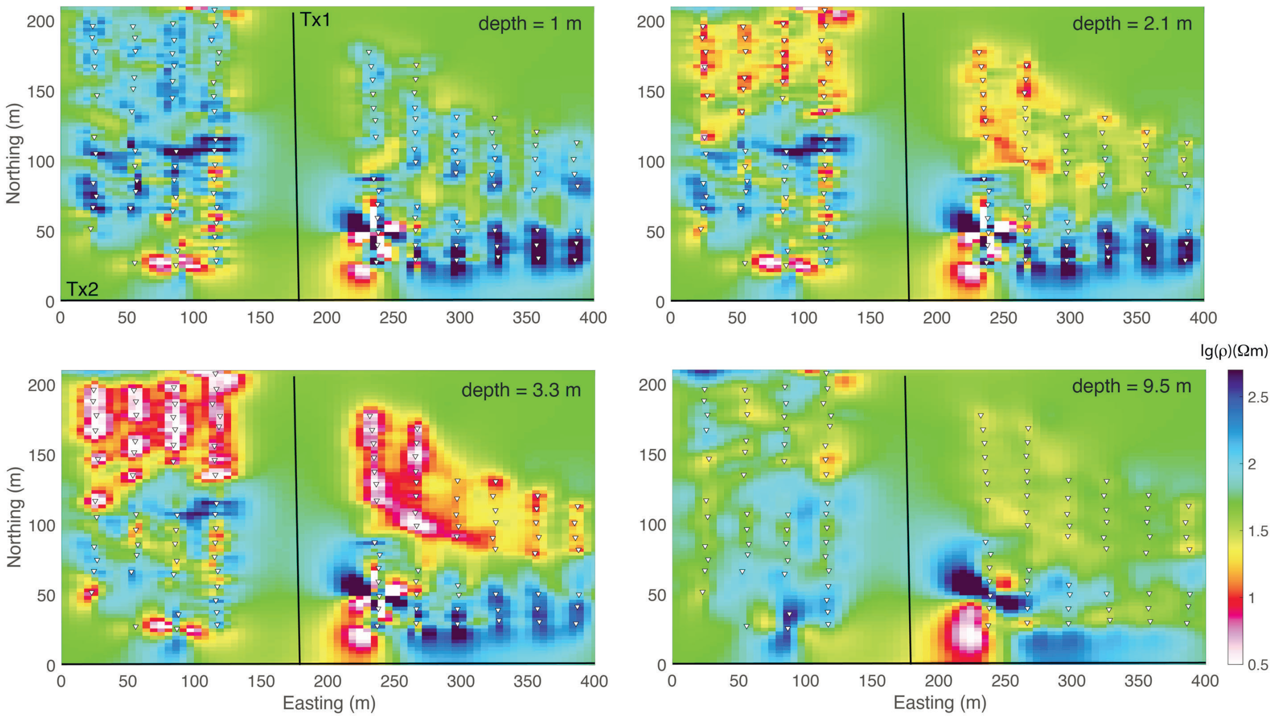

Figure 4. 3-D Weidenpesch waste site model. Horizontal *xy* slices at different depths. Black lines indicate the location of the source, and white triangles – represent sites.